JOC Article

The Recognition and Sensing of Anions through "Positive Allosteric Effects" Using Simple Urea−Amide Receptors

Cidália M. G. dos Santos,[†] Thomas McCabe,[†] Graeme W. Watson,[†,‡] Paul E. Kruger,[§] and Thorfinnur Gunnlaugsson*,[†]

School of Chemistry, Center for Synthesis and Chemical Biology, Trinity College Dublin, Dublin 2, Ireland, School of Chemistry, Trinity College Dublin, Dublin 2, Ireland, and Department of Chemistry, College of Science, University of Canterbury, Christchurch, 8020, New Zealand

gunnlaut@tcd.ie

Received July 2, 2008

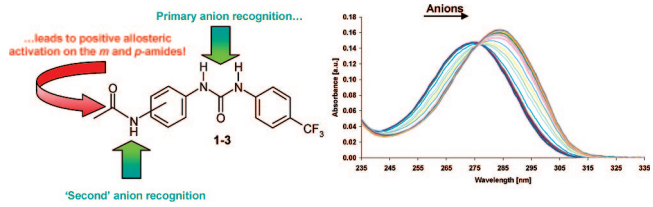

The design, synthesis, and X-ray crystallographic analysis of three simple diaryl-urea based anion receptors possessing an amide moiety on one of the aryl groups, and an electron withdrawing CF_3 group on the other, is described. The three receptors differ only in the position of the amide functionality relative to the hydrogen bonding urea moiety (being *para, meta*, and *ortho* for **1**, **2**, and **3**, respectively). This simple modification was shown to have a significant effect on the anion recognition ability, the strength of the recognition process, and the stoichiometry (host/guest) for these sensors. We demonstrate, by using both UV−vis absorption and ^{1}H NMR spectroscopy, that these factors are caused by the ability of the amide moiety to both modulate the anion binding selectivity and the sensitivity of the urea moiety. We also demonstrate that, in the case of **1** and **2**, this anion recognition at the urea moiety leads to concomitant activation (through enhanced inductive effect) in the amide functionality toward anions, which leads to the formation of an overall 1:2 (sensor/anion) binding stoichiometry for these receptors. This "activation" we describe as being an example of a "positive allosteric activation" by the urea site, caused directly by the first anion binding interaction, which to the best of our knowledge, has not been previously demonstrated for anion recognition and sensing.

Introduction

The design and utility of luminescent and colorimetric molecules for anion recognition and sensing is an active field of research within the area of supramolecular chemistry.[1−3] Initially, anion recognition was predominantly achieved by using charged host molecules, such as protonated polyamines or azamacrocycles,[4] guanadinium[5] or transition metal, or lanthanide ion based complexes.[6] More recently charge neutral receptors such as amides,[7] carbamides,[8] urea and thioureas, [9,10] amidoureas,[11] as well as pyrroles,[12] indoles,[13] calixpyrroles,[14] and caticols[15] have been employed as recognition moieties for

[†] Center for Synthesis and Chemical Biology, Trinity College Dublin.
[‡] School of Chemistry, Trinity College Dublin.
[§] University of Canterbury.

(1) (a) Gunnlaugsson, T.; Glynn, M.; Tocci (née Hussey) , G. M.; Kruger, P. E.; Pfeffer, F. M. *Coord. Chem. Rev.* **2006**, *250*, 3094. (b) Steed, J. W. *Chem. Commun.* **2006**, 2637. (c) Gale, P. A.; Garcia-Garrido, S. E.; Garric, J. *Chem. Soc. Rev.* **2008**, *37*, 151.

(2) (a) Padros P. Quesada, R. *Supramol. Chem* **2008**, *20*, 201. (b) Filby, M. H.; Steed, J. W. *Coord. Chem. Rev.* **2006**, *250*, 3200. (c) Gale, P. A.; Quesada, R. *Coord. Chem. Rev.* **2006**, *250*, 3219. (d) Nguyen, B. T.; Anslyn, E. V. *Coord. Chem. Rev.* **2006**, *250*, 3118. (e) Gunnlaugsson, T.; Ali, H. D. P.; Glynn, M.; Kruger, P. E.; Hussey, G. M.; Pfeffer, F. M.; dos Santos, C. M. G.; Tierney, J. *J. Fluoresc.* **2005**, *15*, 287. (f) Martínez-Máñez, R.; Sancenón, F. *J. Fluoresc.* **2005**, *15*, 267. (g) Gale, P. A. *Chem. Commun.* **2005**, 3761. (h) Martínez-Máñez, R.; Sancenón, F. *Chem. Rev.* **2003**, *103*, 4419.

(3) Sessler, J. L.; Gale, P. A.; Cho, W. S. *Anion Receptor Chemistry*; Royal Society of Chemistry: Cambridge, UK, 2006.

(4) Recent example includes: (a) Nelissen, H. F. M.; Smith, D. K. *Chem. Commun.* **2007**, 3039. Review in: (b) *Supramolecular Chemistry of Anions*; Bianchi, E., Bowman-James, K., Gracía-Españña, E., Eds.; Wiley-VCH: New York, 1997; (c) Choi, K.; Hamilton, A. D. *Coord. Chem. Rev.* **2003**, *240*, 101.

(5) (a) Best, M. D.; Tobey, S. L.; Anslyn, E. V. *Coord. Chem. Rev.* **2003**, *240*, 3. (b) Rozas, I.; Kruger, P. E. *J. Chem. Theory Comput.* **2005**, *1*, 1055.

(6) (a) Gunnlaugsson, T.; Stomeo, F. *Org. Biomol. Chem.* **2007**, *5*, 1999. (b) Leonard, J. P.; Nolan, C. B.; Stomeo, F.; Gunnlaugsson, T. *Top. Curr. Chem.* **2007**, *281*, 1. (c) Gunnlaugsson, T.; Leonard, J. P. *Chem. Commun.* **2005**, 3114. (d) Leonard, J. P.; Gunnlaugsson, T. *J. Fluoresc.* **2005**, *15*, 585.

10.1021/jo8014424 CCC: $40.75
Published on Web 11/06/2008

anions. The use of such versatile synthetic functionalities has enabled the design and construction of more sophisticated anion receptors,[16] which facilitates a more effective targeting approach to anion sensing using arrays of hydrogen bonding donors, where both the selectivity and the sensitivity of the recognition process can be tuned.[17] We have in the past demonstrated that such charge neutral functionalities can be employed in both colorimetric[18,19] and fluorescent[20,21] anion sensing, either in organic solvents such as CH_3CN and DMSO, or in more competitive media such as ethanol and buffered aqueous solution.[5] Recently, amidoureas and thioureas[11] have been incorporated into structurally preorganized hosts which gave rise to both enhanced selectivity and sensitivity for ions such as phosphate and pyrophosphate. While the 'amide' functionality of these systems has been an integrated part of the main "receptor moiety", we demonstrate herein that the introduction of these functional groups into simple anion based diaryl

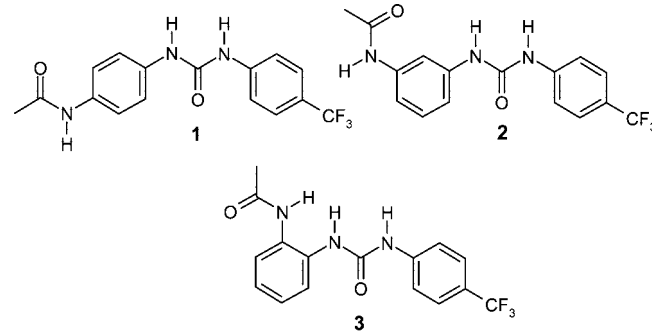

receptors as independent components, **1**−**3** (where the amide is located at the *para, meta* and *ortho* positions, respectively), gives rise to the recognition of several anions with concomitant high binding affinities in CH_3CN. We also demonstrate that the substitution pattern in **1**−**3**, has significant effects on both the sensitivity as well as the stoichiometry of the anion recognition, which was investigated using both UV−vis absorption and ^1H NMR spectroscopy in organic solvents. We demonstrate, for the first time that in the case of **1** and **2**, the binding of anions at the urea moiety, enhances, or activates, the recognition ability of the amide moiety enabling these receptors to bind anions such as acetate in 1:1 as well as in 1:2 binding stoichiometry. Here, the second anion binding at the amide site *only* occurs after this primary recognition at the urea site takes place. This phenomenon we like to describe as being an example of a "positive allosteric effect"[22a] caused by the first anion binding event.[22b,c] In comparison, **3** only gave the 1:1 binding stoichiometry, where the amide moiety cooperatively participated in the initial anion binding event at the urea site. Hence, this location prevents any "allosteric activation" caused by the first anion binding. To the best of our knowledge, this is the first time that such effects have been employed for the sensing of anions using urea based receptors.[22d] Consequently, the results presented herein open up a new avenue for the design of anion targeting receptors. Herein, we describe the synthesis and the characterization of **1**−**3**, which includes the analysis of their X-ray crystal structures and packing in the solid state, as well as their ability to bind anions in the manner outlined above.

Results and Discussion

Synthesis and X-Ray Crystallographic Analysis of 1−3. The synthesis of compounds **1**−**3** is shown in Scheme 1. Using the commercially available nitroanilines **4**−**6** (the para, *meta* and *ortho* isomers, respectively), the amino groups were converted to the corresponding amides **7**−**9**, by reacting **4**−**6** in neat acetic anhydride at room temperature overnight. The resulting off-white colored precipitates were collected by filtration and each batch washed twice with diethyl ether and dried under high vacuum, giving **7**−**9** in 83, 57 and 57% yields, respectively. Reduction of the nitro groups in **7**−**9** using hydrazine monohydrate and 10% Pd/C in ethanol under reflux for 12 h, gave **10**−**12** as off-white solids in almost quantitative

(7) (a) Kang, S. O.; Begum, R. A.; Bowman-James, K. *Angew. Chem., Int. Ed.* **2007**, *45*, 7882. (b) Kang, S. O.; Hossain, Md. A.; Bowman-James, K. *Coord. Chem. Rev.* **2006**, *250*, 3038. (c) Goetz, S.; Kruger, P. E. *Dalton Trans.* **2006**, 1277.

(8) (a) Davis, A. P. *Coord. Chem. Rev.* **2006**, *250*, 2939. (b) Davis, A. P.; Joos, J. B. *Coord. Chem. Rev.* **2003**, *240*, 143.

(9) Gunnlaugsson, T.; Kruger, P. E.; Jensen, P.; Tierney, J.; Ali, H. D. P.; Hussey, G. M. *J. Org. Chem.* **2005**, *70*, 10875.

(10) (a) Pescatori, L.; Arduini, A.; Pochini, A.; Ugozzoli, F.; Secchi, A. *Eur. J. Org. Chem.* **2008**, 109. (b) Wang, H.; Chan, W.-H. *Org. Biol. Chem.* **2008**, *6*, 162. (c) Chawla, H. M.; Singh, S. P. *Tetrahedron* **2008**, *64*, 741. (d) Kumar, M.; Babu, J. N.; Bhalla, V.; Athwal, N. S. *Supramol. Chem.* **2007**, *19*, 511. (e) Lin, C.; Simov, V.; Drueckhammer, D. G. *J. Org. Chem.* **2007**, *72*, 1742. (f) Evans, L. S.; Gale, P. A.; Light, M. E.; Quesada, R. *New. J. Chem.* **2006**, *30*, 1019. (g) Brooks, S. J.; Gale, P. A.; Light, M. E. *Chem. Commun.* **2006**, 4344. (h) Gunnlaugsson, T.; Pfeffer, F. M.; Buschgens, A. M.; Barnett, N. W.; Gunnlaugsson, T.; Kruger, P. E. *Tetrahedron Lett.* **2005**, *46*, 6579. (i) Gunnlaugsson, T.; Davis, A. P.; O'Brien, J. E.; Glynn, M. *Org. Biomol. Chem.* **2005**, *3*, 48. (j) Gunnlaugsson, T.; Davis, A. P.; Hussey, G. M.; Tierney, J.; Glynn, M. *Org. Biomol. Chem.* **2004**, *2*, 1856. (k) Boiocchi, M.; Boca, L. D.; Gómez, D. E.; Fabbrizzi, L.; Licchelli, M.; Monzani, E. *J. Am. Chem. Soc.* **2004**, *126*, 16507. (l) Kato, R.; Cui, Y.-Y.; Nishizawa, S.; Yokobori, T.; Teramae, N. *Tetrahedron Lett.* **2004**, *45*, 4273. (m) Jose, D. A.; Kumar, D. K.; Ganguly, B.; Das, A. *Org. Lett.* **2004**, *6*, 3445. (n) Gunnlaugsson, T.; Davis, A. P.; O'Brien, J. E.; Glynn, M. *Org. Lett.* **2002**, *4*, 2449. (o) Davis, A. P.; Glynn, M. *Chem. Commun.* **2001**, 2556. (p) Wel, L. H.; He, Y. B.; Wu, J. L.; Wu, X. J.; Meng, L.; Yang, X. *Supramol. Chem.* **2004**, *16*, 561.

(11) (a) Yang, R.; Liu, W.-X.; Shen, H.; Huang, H.-H.; Jiang, Y.-B. *J. Phys. Chem. B* **2008**, *112*, 5105. (b) Liu, W.-X.; Jiang, Y.-B. *Org. Biomol. Chem.* **2007**, *5*, 1771. (c) Quinlan, E.; Matthews, S. E.; Gunnlaugsson, T. *Tetrahedron Lett.* **2006**, *47*, 9333. (d) Evans, L. S.; Gale, P. A.; Light, M. E.; Quesada, R. *Chem. Commun.* **2006**, 965. (e) Wu, F. Y.; Li, Z.; Guo, L.; Wang, X.; Lin, M. H.; Zhao, Y. F.; Jiang, Y. B. *Org. Biomol. Chem.* **2006**, *4*, 624. (f) Nei, L.; Li, Z.; Han, J.; Zhang, X.; Yang, R.; Liu, W.-X.; Wu, F.-Y.; Xie, J.-W.; Zhao, Y.-F.; Jiangm, Y.-B. *J. Org. Chem.* **2004**, *69*, 6449.

(12) (a) Brooks, S. J.; Edwards, P. R.; Gale, P. A.; Light, M. E. *New J. Chem.* **2006**, *30*, 65. (b) Camiolo, S.; Gale, P.; Hursthouse, M. B.; Light, M. E. *Org. Biomol. Chem.* **2003**, *1*, 741.

(13) (a) Pfeffer, F. M.; Lim, K. F.; Sedgwick, K. J. *Org. Biomol. Chem.* **2007**, *5*, 1795. (b) Bates, G. W.; Triyanti, Light, M. E.; Albrecht, M.; Gale, P. A *J. Org. Chem.,* **2007**, *72*, 8921.

(14) Sessler, J. L.; Davis, J. M. *Acc. Chem. Res.* **2001**, *34*, 989.

(15) Winstanley, K. J.; Smith, D. K. *J. Org. Chem.* **2007**, *72*, 2803.

(16) O'Neil, E. J.; Smith, B. D. *Coord. Chem. Rev.* **2006**, *250*, 3068.

(17) Gale, P. A. *Acc. Chem. Res.* **2006**, *39*, 465.

(18) Quinlan, E.; Matthews, S. E.; Gunnlaugsson, T. *J. Org. Chem.* **2007**, *72*, 7497.

(19) (a) Ali, H. D. P.; Kruger, P. E.; Gunnlaugsson, T. *New. J. Chem.* **2008**, *32*, 1153. (b) Pfeffer, F. M.; Kruger, P. E.; Gunnlaugsson, T. *Org. Biomol. Chem.* **2007**, *5*, 1894.

(20) (a) Duke, R. M.; Gunnlaugsson, T. *Tetrahedron Lett.* **2007**, *48*, 8043. (b) dos Santos, C. M. G.; McCabe, T.; Gunnlaugsson, T. *Tetrahedron Lett.* **2007**, *48*, 3135.

(21) Recent example includes: dos Santos, C. M. G.; Glynn, M.; McCabe, T.; de Melo, J. S. S.; Burrows, H. D.; Gunnlaugsson, T. *Supramol. Chem.* **2008**, *20*, 407.

(22) (a) The field of "Allosteric Supramolecular Receptors and Catalysts" has recently been reviewed by Kovbasyuk, L.; Krämer, R. *Chem. Rev.* **2004**, *104*, 3161. (b) Ercolani has recently reviewed and examined the cause of cooperatively in self-assembly formations in supramolecular chemistry Ercolani, G. *J. Am. Chem. Soc.* **2003**, *125*, 16097. While our results do not strictly fulfill the criteria set out in this publication for *positive cooperativity*, the results demonstrate that only after the first binding at the urea moiety is the binding of the amide activated in compounds **1** and **2**. While this is most likely the cause of enhanced inductive effect as the result of the first anion binding (caused by enhanced ICT within the molecule), we proposed that this "mechanism" for anion recognition can be described as an example of positive allosteric effect. (c) Other example includes: Deetz, M. J.; Smith, B. D. *Tetrahedron Lett.* **1998**, *39*, 6841. (d) Recently, pyridyl thioureas were developed as switchable anion receptors by Kilburn et al.: Rashdan, S.; Leight, M. E.; Kilburn, J. D. *Chem. Commun.* **2006**, 4578.

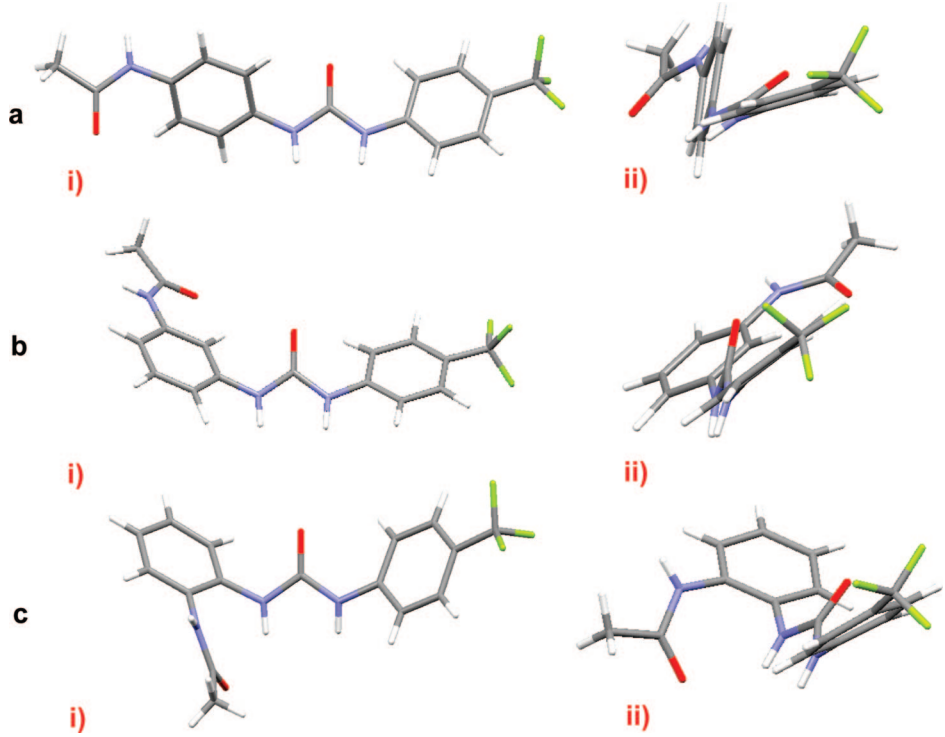

FIGURE 1. X-ray crystal structures of compounds **1**−**3** (a−c, respectively) as viewed: (i) side on and (ii) by viewing the relative tilt in the two aryl groups around the urea moiety.[23]

yields for **1** and **3**, while compound **2** was formed in 58% yield. The anion receptors **1**−**3** were then formed by reacting **10**−**12** in $CHCl_3$ with trifluoro-*p*-tolyl isocyanate at room temperature overnight under an atmosphere of argon. The resulting precipitates were filtered and washed with cold $CHCl_3$ and collected to give **1**−**3** in 90, 70 and 88% yield, respectively. All three receptors were fully characterized using conventional techniques for instance, the ^{1}H NMR spectra (400 MHz, DMSO-d_6) showed the presence of the two urea and the amide protons, occurring at 9.87, 9.05 and 8.71 ppm, respectively, for **1**. Similar results were seen for **2** and **3** (see Experimental Section and Figure S1−S4, Supporting Information).

SCHEME 1. Synthesis of Compounds 1−3

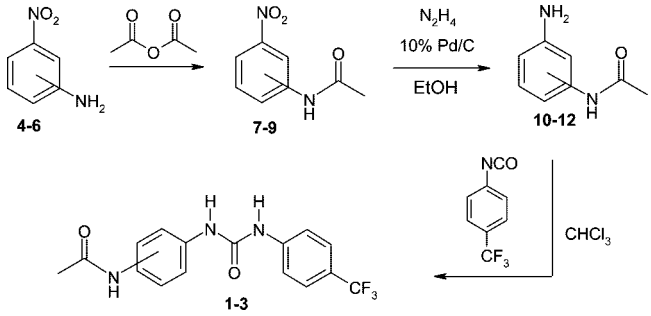

The three receptors were all formed as crystalline materials, and suitable crystals for X-ray crystallographic analysis were, in the case of **1** and **3**, obtained from a mixture of $CHCl_3$ and MeOH at room temperature and from cold $CHCl_3$ in the case of **2**. The X-ray crystal structures of **1**−**3** are shown in Figure 1a−c, which shows that the location of the amide moiety has significant effect on the structure of the bis-aryl receptor (See experimental section and Supporting Information for details).[23] In the case of both **1** and **3**, the two aryl moieties are significantly deconjugated from the central urea, and only for **2**, are the two aryl rings close to being coplanar. In fact, for receptor **1**, the two aryl groups are close to be orthogonal to each other, with a torsion angle of −133.14°, while for **3**, a torsion angle of −118.26° (see Supporting Information) was measured. All the trifluoro-*p*-tolyl groups were also found to be twisted out of the plane of the urea moiety, with torsion angles of −22.67, −38.57 and −42.83 for **1**−**3**, respectively. Of the three receptors, only **3** gives rise to any intramolecular interaction between the two receptors (e.g., the urea and the amide), where a clear hydrogen bond interaction exists between the amide oxygen and one of the urea protons, with O···H distance of 2.18 Å. Similarly, the urea protons hydrogen bond to the amide oxygen with an average O···H bond distance of 2.94 Å. All three structures gave rise to extended intermolecular hydrogen bonding networks, which are commonly found for such aryl-ureas as well as face to face $\pi-\pi$ interactions,[24] which were particularly pronounced in the crystal structures of **1** and **2**. For receptor **1**, the structure, Figure 2, consisted of alternative head-to-tail network, where each of the amide protons were hydrogen bonding to the oxygen of the urea moiety of another molecule, with an average O···H bond length of 2.95 Å. However, the most flattened conformation of the three ligands, **2**, gave rise to tape or ribbon like structures where each of the urea protons were hydrogen bonding in an intermolecular fashion to an oxygen of another urea moiety, with average

(23) *Software Reference Manual*, version 5.625; Bruker Analytical X-Ray Systems Inc.: Madison, WI, 2001. Sheldrick, G. M. *SHELXTL, An Integrated System for Data Collection, Processing, Structure Solution and Refinement*; Bruker Analytical X-Ray Systems Inc.: Madison, WI, 2001. See also Figures S29−S31, Supporting Information.

(24) Custelcean, R. *Chem. Commun.* **2008**, 295.

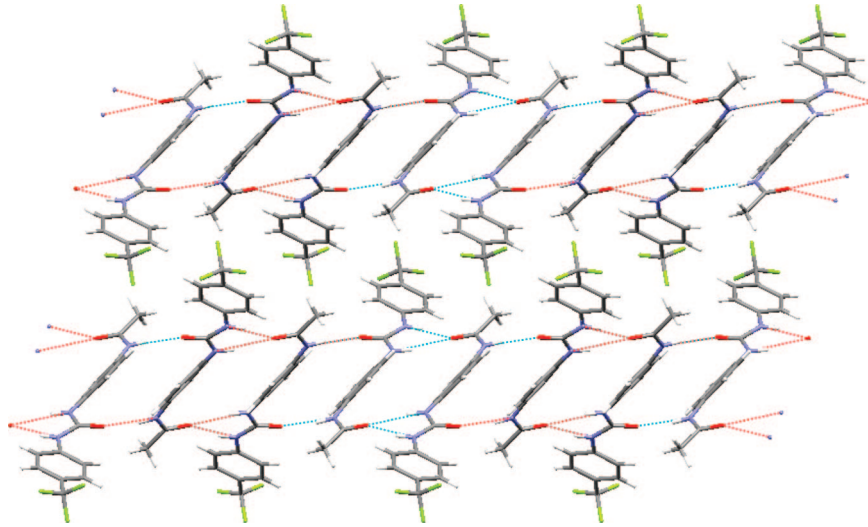

FIGURE 2. Packing diagram of **1** showing the intermolecular hydrogen bonding network that exists between the amide protons and the urea oxygen, when viewed down the crystallographic *b* axis.

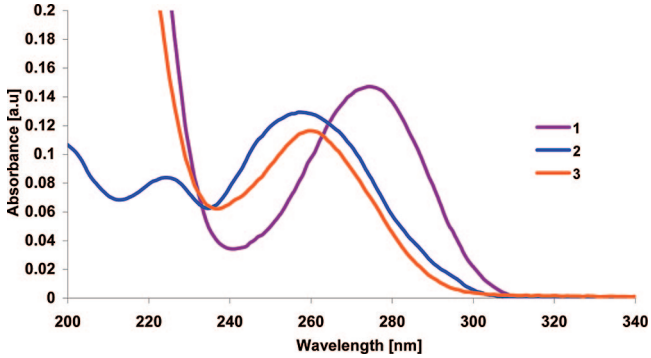

FIGURE 3. Absorption spectra of **1**−**3** when recorded in CH_3CN.

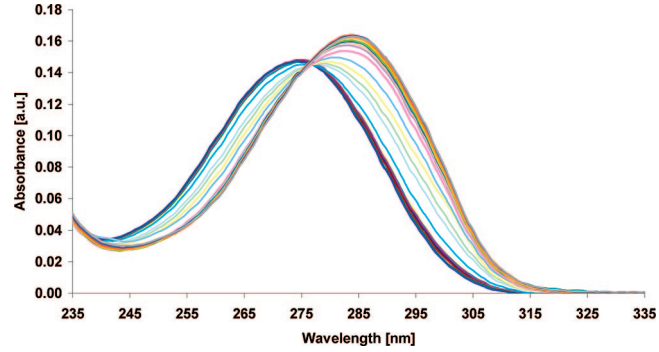

FIGURE 4. Changes in the absorption spectra of **1** (4 μM) upon titration with $H_2PO_4^-$ (0 → 1.63 mM) in CH_3CN.

O···H distance of 2.89 Å (Figure S5, Supporting Information). No clear hydrogen bonding interactions were observed for the amide functionality of **2**, which did not seem to participate in either intra- or intermolecular hydrogen bonding interactions. In contrast to these results, **3** (Figure S6, Supporting Information), gave rise to complicated packing network which was consisted of both intra- and intermolecular hydrogen bonding interactions. With the aim of investigating both the mode of the anion binding and the effect such binding had on the solid state packing of these receptors, an attempt was made to grow crystals of all three receptors with a variety of anions, using several types of solvents, by growing these complexes using slow diffusion, layering or slow evaporation. Unfortunately, all of these failed to generate suitable crystals for crystal structure analysis.

Anion Binding Studies of 1−3 using UV−Vis Absorption Titrations. The absorption spectra of **1**−**3**, when recorded at room temperature in CH_3CN, are shown in Figure 3. Receptors **1** and **3** exhibited a broadband centered at *ca.* 274 nm (log $\varepsilon = 4.57$) and *ca.* 260 nm (log $\varepsilon = 4.46$), respectively, assigned to their $\pi-\pi^*$ transitions. Receptor **2** showed the presence of a broadband centered at *ca.* 257 nm (log $\varepsilon = 4.50$), assigned to the $\pi-\pi^*$ transitions, as well as a smaller band at *ca.* 224 nm (log $\varepsilon = 4.31$). The significant 17−20 nm difference in the λ_{max} of **1** to that of **2** or **3** can be attributed to the relative location of the amide to that of the urea moiety, and possible weak internal charge transfer (ICT) contribution. Upon excitation at their relevant λ_{max} wavelengths, all ligands gave rise to only weak fluorescence. Consequently, only the ground-state changes were investigated in depth upon binding of these receptors to anions, the results of which will be discussed below.

With the aim of evaluating both the anion binding ability of **1**−**3** (4 μM each) and the stoichiometries for the resulting binding interactions, all were titrated with acetate (AcO^-), dihydrogenphosphate ($H_2PO_4^-$), dihydrogenpyrophosphate ($H_2P_2O_7^{2-}$), fluoride (F^-), and chloride (Cl^-) in CH_3CN as their tetrabutylammonium salts (TBA^+). The changes in the absorption spectra of **1** for the titration with $H_2PO_4^-$ are presented in Figure 4, and clearly demonstrate significant changes upon binding of **1** with the anion. Here, the band centered at *ca.* 274 nm was red-shifted to *ca.* 284 nm with the formation of an isosbestic point at *ca.* 276 nm. The same behavior was observed for $H_2P_2O_7^{2-}$, while both AcO^- and F^- exhibited the bigger shifts, *ca.* 286 nm and *ca.* 287 nm, respectively (see Figure S7−S9, Supporting Information). The observed changes constitute evidence for the hydrogen bonding interactions between **1** and these particular anions. Moreover, upon adding competitive solvents such as MeOH or H_2O to solutions of **1** bound to these anions, the spectral changes were reversed, indicating that the recognition process was reversible. In contrast to the above results, the spectral changes observed for Cl^- were, however, less significant and occurred only at a relatively higher concentration of the anion (Figure S10, Supporting Information). From these absorption changes the binding constants (expressed as log *K*) for the complex formation between the anions (**G**)

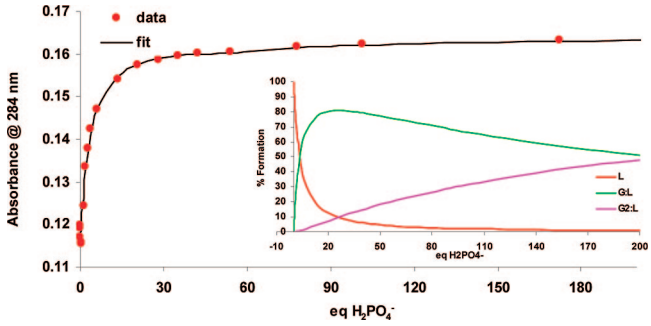

FIGURE 5. Experimental binding isotherm for the absorption titration of **1** (**L**) (4 μM) with $H_2PO_4^-$ (**G**) (and the corresponding fit from SPECFIT). (Inset) Speciation distribution diagram for the same titration.

TABLE 1. Binding Constants and Binding Stoichiometries Obtained for the Anion Titrations of 1 Using the SPECFIT Program

anion (**G**)	binding mode ($\mathbf{G_n}$:$\mathbf{L_m}$)	log $K_{n:m}$	std. deviation
AcO^-	**G**:**L**	5.29	0.03
	$\mathbf{G_2}$:**L**	3.50	0.19
F^-	**G**:**L**	5.25	0.05
	$\mathbf{G_2}$:**L**	2.72	0.23
$H_2PO_4^-$	**G**:**L**	4.93	0.05
	$\mathbf{G_2}$:**L**	3.08	0.43
$H_2P_2O_7^{2-}$	**G**:**L**	5.88	0.09
Cl^-	**G**:**L**	3.45	0.06

and **1** (**L**) were determined by fitting the data using the nonlinear least-squares regression program SPECFIT. The changes observed in the absorption spectra of **1** at 284 nm, upon binding to $H_2PO_4^-$, and the resulting fit, are shown in Figure 5, and the obtained binding stoichiometries and the resulting log K values are listed in Table 1. As can be seen from Figure 5, an excellent fit was obtained for the changes observed in Figure 4. From these changes two binding constants were determined, where the 1:1 stoichiometry resulted in a log $K_{1:1}$ = 4.93 (±0.05), which was assigned to the binding of $H_2PO_4^-$ at the urea moiety. The second binding interaction was also quite strong and determined to be the result of a 1:2 stoichiometry between **1** and $H_2PO_4^-$, with a log $K_{1:2}$ = 3.08 (±0.43). The speciation distribution diagram for these interactions is shown as insert in Figure 5, and demonstrates that the 1:1 binding between $H_2PO_4^-$ and **1** is fully achieved within the addition of 20 equivalents of the anion. Nevertheless, at higher concentrations (>20 equivalents), the 1:2 stoichiometry becomes stronger, at the expense of the 1:1 stoichiometry; which eventually becomes the dominant species in solution (not shown in full in Figure 5). Such binding interaction could only possibly occur through the vacant amide moiety, *para* to the urea moiety, in a manner shown in Figure 6, as **Form A**. This is a 'single point' interaction between the amide and the anion and hence, would not be expected to give rise to such a relatively strong binding constant. However, recently, Hay et al. have demonstrated that aryl protons in such highly polarizable aromatic rings, can participate in hydrogen bonding to anions.[25] Hence, it is also possible that $H_2PO_4^-$ binds in such a manner, as depicted as **Form B** in Figure 6. Furthermore, in a related anion binding study carried out within our laboratory, using a urea analogue of **1**, where the amide was replaced by an electron withdrawing fluoride substituents, then in DMSO solution, only the 1:1 binding stoichiometry was observed (log K = 3.69), and no evidence of 1:2 binding was

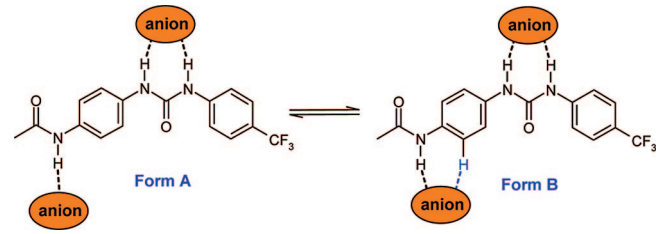

FIGURE 6. Possible 1:2 binding of $H_2PO_4^-$ to **1**, where each anion has two binding locations.

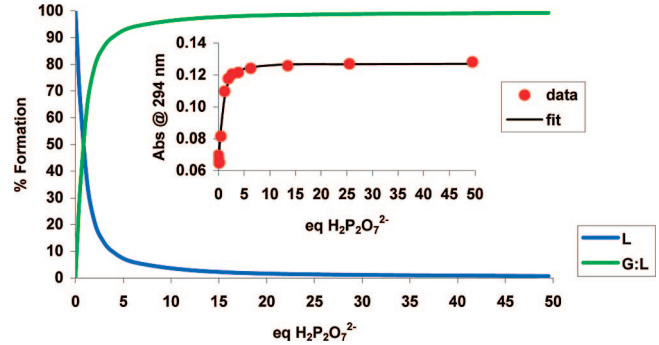

FIGURE 7. Speciation distribution diagram for the titration of **1** (**L**) with $H_2P_2O_7^{2-}$ (**G**) in CH_3CN. Speciation is shown relative to the number of equivalents of $H_2P_2O_7^{2-}$. (Inset) Fit to the experimental binding isotherm obtained using SPECFIT.

observed. This clearly indicates that the amide function is indeed participating in hydrogen binding interaction with the anion in **1**.

In a similar manner, both AcO^- and F^- exhibited a similar binding trend, where the 1:1 binding stoichiometry dominated initially, with log $K_{1:1}$ values of 5.29 and 5.25, respectively, with the formation of the 1:2 binding stoichiometry at higher concentrations (see Figure S11 and S12, Supporting Information). These constants are marginally greater than those determined for $H_2PO_4^-$, demonstrating higher affinities of **1** for these anions. Such binding selectivity has previously been observed for such urea or thiourea binding moieties.[9] The 1:2 binding was also observed, being determined as log $K_{1:2}$ = 3.50 (±0.19) and log $K_{1:2}$ = 2.72 (±0.23) for AcO^- and F^-, respectively. When these titrations were repeated using $H_2P_2O_7^{2-}$ or Cl^-, only the 1:1 binding was observed for both anions. In the case of the divalent $H_2P_2O_7^{2-}$ anion, both an excellent fit, Figure 7, and a very strong binding interaction were observed, with log $K_{1:1}$ = 5.88 (±0.09). The above binding values are summarized in Table 1.

Having established the anion binding ability of **1**, we next turned out attention to the structural isomer **2**. Upon addition of anions such as $H_2PO_4^-$ (Figure S13, Supporting Information) or AcO^-, Figure 8, the absorption spectrum of **2** was also bathochromically shifted, with the formation of an isosbestic point at 265 nm. As observed for **1**, fitting these changes, showed the presence of two new host:guest complexes in solution; namely the 1:1 species, which was formed at low concentration of the anion, with a log $K_{1:1}$ = 5.41 (±0.02), and the formation of the 1:2 binding stoichiometry, which was formed with log $K_{1:2}$ = 3.06 (±0.38). While the former of these is comparable to that observed for the 1:1 binding of **1**, the 1:2 binding affinity is somewhat reduced.

(25) (a) Hay, B. P.; Friman, T. K.; Moyer, B. A. *J. Am. Chem. Soc.* **2005**, *127*, 1810. See also: (b) Kwon, J. Y.; Jang, Y. J.; Kim, S. K.; Lee, K.-H.; Kim, J. S.; Yoon, J. *J. Org. Chem.* **2004**, *69*, 5155.

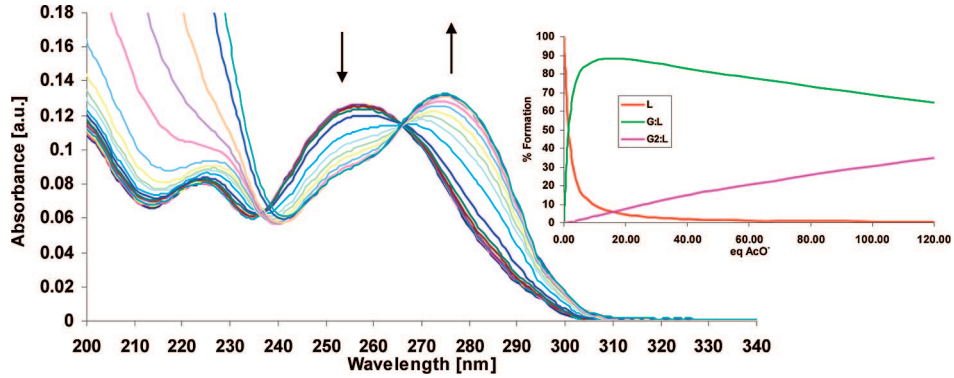

FIGURE 8. Changes in the absorption spectrum of **2** (4 μM) upon titration with AcO^- (0 → 0.77 mM) in CH_3CN. (Inset) Speciation distribution diagram for same titration of **2** (**L**) and AcO^- (**G**).

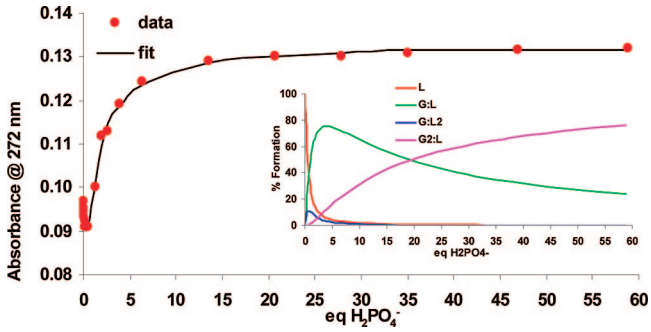

FIGURE 9. Data obtained at 272 nm and the corresponding fit using the SPECFIT program for the titration of **2** (4 μM) using $H_2PO_4^-$ (0 → 0.235 mM). (Inset) Speciation distribution diagram for the binding of $H_2PO_4^-$.

TABLE 2. Binding Constants and Binding Modes Obtained for the Anion Titrations of 2 Using the SPECFIT Program

anion (**G**)	binding mode ($\mathbf{G_n}$:$\mathbf{L_m}$)	log $K_{n:m}$	std. deviation
AcO^-	**G**:**L**	5.41	0.02
	$\mathbf{G_2}$:**L**	3.06	0.38
F−	**G**:**L**	6.13	0.09
	G:$\mathbf{L_2}$	5.48	0.29
	$\mathbf{G_2}$:**L**	3.29	0.26
$H_2PO_4^-$	**G**:**L**	6.05	0.07
	G:$\mathbf{L_2}$	5.30	0.26
	$\mathbf{G_2}$:**L**	4.15	0.12
$H_2P_2O_7^{2-}$	**G**:**L**	3.54	0.21
	G:$\mathbf{L_2}$	6.06	0.19
	$\mathbf{G_2}$:**L**	4.04	0.14
Cl^-	**G**:**L**	4.86	0.09
	G:$\mathbf{L_2}$	6.42	0.21

The titration of **2** with $H_2PO_4^-$ gave rise to similar spectral results (Figure S11, Supporting Information), where the band centered at *ca.* 224 nm was shifted to *ca.* 227 nm with the formation of a clear isosbestic point at *ca.* 236 nm, while the band centered at *ca.* 257 nm experienced a bigger shift to *ca.* 272 nm. This shift was also accompanied with the formation of an isosbestic point at *ca.* 263 nm. However, unlike that seen for either AcO^- or $H_2PO_4^-$, both of which gave rise to 1:1 and 1:2 binding with **1**, the changes observed here, were best fitted to 1:1, 2:1 and 1:2 stoichiometries, as shown in Figure 9. Nevertheless, the formation of the 1:1 stoichiometry was still the most dominant species in solution, being initially formed with a much smaller contribution from the 2:1 stoichiometry. As was observed above for **1**, the formation of the 1:2 species became dominant only at high equivalents of AcO^-. Similar behavior was also observed for F^- and pyrophosphate (Figure S14 and S15, Supporting Information) which exhibited shifts to 274 nm with the appearance of an isosbestic point at 266 nm. In contrast to this, spectral changes observed induced by Cl^- only occurred at relatively higher concentration of the anion, and these were also the smallest among the anions studied, of *ca.* 12 nm, which nevertheless, was larger than that observed for **1** of 6 nm (Figure S16, Supporting Information) for Cl^-. However, significant changes were also observed at shorter wavelengths that were not present to the same extend in the other titrations.

Analysis of all the changes discussed above, using the SPECFIT program allowed for the determination of the binding affinity of these anions for **2**. These results are summarized in Table 2, and demonstrate that in comparison with **1**, receptor **2** displayed a more intricate behavior, where F^- and $H_2PO_4^-$ exhibited the largest binding constants for the 1:1 interaction with log $K_{1:1}$ = 6.13 (±0.09) and log $K_{1:1}$ = 6.05 (±0.07), respectively. Furthermore, AcO^- gave rise to significantly higher 1:1 binding to **2**, while only for $H_2P_2O_7^{2-}$ was the 1:1 binding to **2** weaker than observed for **1**, with $K_{1:1}$ = 3.54 (±0.21). However, the 2:1 binding constant for $H_2P_2O_7^{2-}$, was significantly stronger with a log $K_{1:2}$ = 6.06 (±0.19). In contrast to these results, both F^- and $H_2PO_4^-$exhibited similar binding constants for the 1:2 binding stoichiometry as seen for **1** above, with log $K_{1:2}$ = 5.48 (±0.29) and log $K_{1:2}$ = 5.30 (±0.26), respectively.

In general, it can be assumed that the 1:1 binding was stronger for **2** then observed for **1**, and on all occasions, a small contribution from the 2:1 (host:guest) binding was also observed. Furthermore, only for the exception of AcO^-, did the 1:1 binding stoichiometry result in higher binding constants for **2** than **1**. This is possibly due to the stronger resonance effects, for **2** than **1** (i.e., *meta* vs *para*), causing the amide moiety to become more electron withdrawing due to the presence of the urea moiety. The fact that in these structures a single amide is able of participating in "independent" binding of the anion, with such high binding affinity, is very interesting, as generally a single amide moiety would not be expected to form such strong hydrogen bonding interactions with anions.[7] Hence, for structure **1** and **2**, we propose that upon anion recognition at the urea moiety, the resulting host:guest complex activates its hydrogen bonding ability of the amide and hence positive allosteric effect (possibly caused by enhanced inductive effect), and the second anion recognition becomes more prominent.

Unlike either **1** or **2**, receptor **3** offers the possibility of direct cooperative binding between the amide and the urea functionality due to the close proximity of these hydrogen bonding donors.

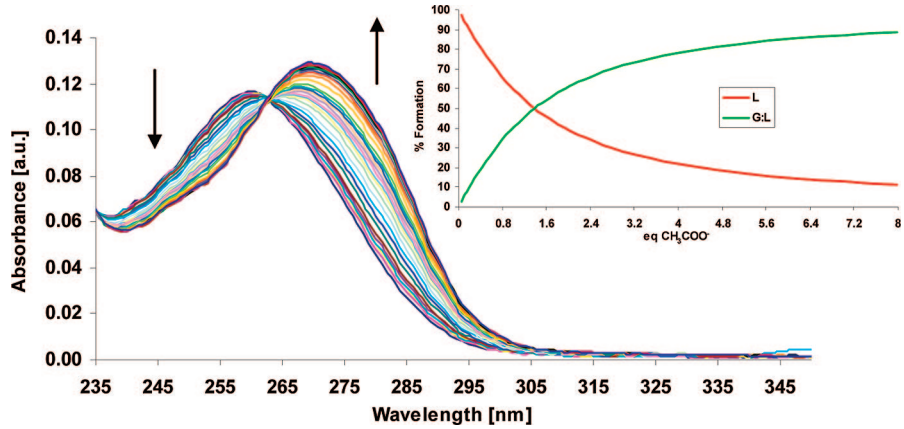

FIGURE 10. Changes in the absorption spectra of **3** (4 μM) upon titration with AcO^- (0 − 32 μM) in CH_3CN. (Inset) Speciation distribution diagram for the same titration of **3** (**L**) with AcO^- (**G**).

TABLE 3. Binding Constants and Binding Modes Obtained for the Anion Titrations of 3 Using the SPECFIT Program

anion (**G**)	binding mode ($\mathbf{G_n}$:$\mathbf{L_m}$)	log $K_{n:m}$	std. deviation
AcO^-	**G**:**L**	5.45	0.02
F^-	**G**:**L**	5.63	0.05
$H_2PO_4^-$	**G**:**L**	5.72	0.05
$H_2P_2O_7^{2-}$	**G**:**L**	6.46	0.06
Cl^-	**G**:**L**	3.60	0.05

This was clear from the X-ray crystal structure in Figure 1c. Upon addition of AcO^-, the absorption band centered at *ca.* 260 nm was once again, red-shifted, to 270 nm, with the concomitant formation of an isosbestic point at 262nm, Figure 10. Similar behavior was observed for **3** to that seen above for **1** and **2**, for all the anions studied (Figure S17−S20, Supporting Information). Once more, the smallest spectral changes were seen for Cl^-, where the 260 nm band was red shift to *ca.* 264 nm, with the appearance of an isosbestic point at *ca.* 262 nm. On all occasions, excellent fit was observed for the experimental binding isotherm (See Figure S17−S20, Supporting Information), when these changes were analyzed using the SPECFIT program. However, unlike that seen above, only the 1:1 binding interaction was observed for the titration of **3** with AcO^-, as demonstrated as insert in Figure 10. This clearly confirms that the amide function was not free to participate in anion recognition in a manner observed for **1** and **2**, suggesting that the amide is participating directly in cooperative anion binding at the urea moiety.

Analysis of the data indeed demonstrated that the binding constants, as summarized in Table 3, where all quite large at the same time as being very similar. Nevertheless, the $H_2PO_4^-$ was stronger than the binding of AcO^-, and of similar magnitude to that seen for **1** for the 1:1 binding to $H_2PO_4^-$. As predicted, Cl^- was found in comparison to interact only weakly with **3** with a binding constant of 3.60 (±0.05). The stronger interaction was observed for $H_2P_2O_7^{2-}$ with a binding constant of 6.46 (±0.06), which is significantly higher than observed for either **1** or **2**. Interestingly, unlike that observed for either **1** or **2**, the binding of F^- was only observed as being in 1:1 stoichiometry, suggesting that the relative orientation of the two anion receptors prevents deprotonation from occurring.

^{1}H NMR Analysis of 1−3 on the Binding of Various Anions. As detailed above, the interactions of **1**−**3** with anions was through hydrogen bonding, with the exception of F^-, where the combinations of hydrogen bonding and deprotonation can also occur. With the aim of further evaluating these binding interactions, and to determine if positive allosteric binding activation occurred after the first binding event at the urea moiety, we carried out detailed ^{1}H NMR titrations of **1**−**3** in DMSO-d_6 (which shows the three N−H resonance more clearly than in CD_3CN) observing the changes in the two urea and the amide protons upon the recognition of anions. The stack plot of the ^{1}H NMR spectra of **2** upon addition of various equivalents of AcO^- is shown in Figure 11 (see Figure S21 and S22 for **1** and **3**, respectively, Supporting Information) and clearly illustrates the dramatic changes observed in the structure of **2**, and in particularly, the significant downfield shifts experienced by the urea protons (H1 and H2) upon binding to AcO^-. Such large downfield shifts/changes have been seen previously for such diaryl urea and thiourea based receptors, and usually signify strong association.[26] In contrast, the changes in the amide proton (H3) were significantly smaller, however, the binding of AcO^- also lead to drastic changes in the aromatic protons, which became much more resolved, or desymmetrized.

With the aim of analyzing these changes further, the changes in the urea resonances ($\Delta\delta$) were plotted against the equivalents of anion added, Figure 12. For the urea protons (H1 and H2), the major changes occurred within 0→1 equivalents of AcO^-, Figure 12a, with no significant changes occurring thereafter. This is in agreement with the formation of a 1:1 binding stoichiometry between the urea acceptor and AcO^-. In contrast, the changes in the amide proton, initially appearing at 9.95 ppm, are very different, as within the 0→1 equivalent, the amide proton is only slightly upfield shifted, Figure 12b. This we assign to the effect caused by the binding of AcO^- at the urea binding site, however, beyond one equivalent of AcO^-, additional changes occur in the NMR for the amide proton, which is now shifted downfield as a function of increased AcO^- concentration, Figure 12b. This second change, we propose is due to direct hydrogen bonding interactions occurring between the H3 proton and the anion, which confirms the results discussed above in the absorption spectra, that he H3 becomes activated after the initial anion binding at the urea site. Hence, this further demonstrates anion recognition via positive allosteric effect. It is also clear from Figure 12b, that this binding is significantly weaker than that observed for the initial 1:1 binding stoichiometry. These changes were fully reproducible, and support our

(26) (a) Lowe, A. J.; Dyson, G. A.; Pfeffer, F. M. *Eur. J. Org. Chem.* **2008**, 1559. (b) Lowe, A. J.; Dyson, F. A.; Pfeffer, F. M. *Org. Biomol. Chem.* **2007**, *5*, 1343. (c) Pfeffer, F. M.; Gunnlaugsson, T.; Jensen, P.; Kruger, P. E. *Org. Lett.* **2005**, *7*, 5357.

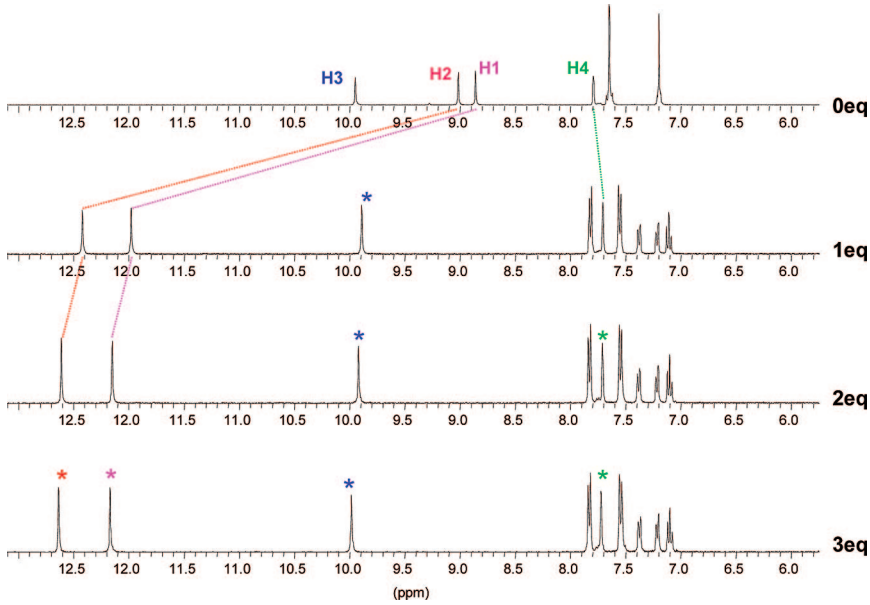

FIGURE 11. Stack plot of the ^{1}H NMR (400 MHz, DMSO-d_6) spectra of **2** upon addition of 0, 1, 2 and 3 equivalents of AcO^-. H1−H3 are the N−H protons. H4 is an aryl proton.

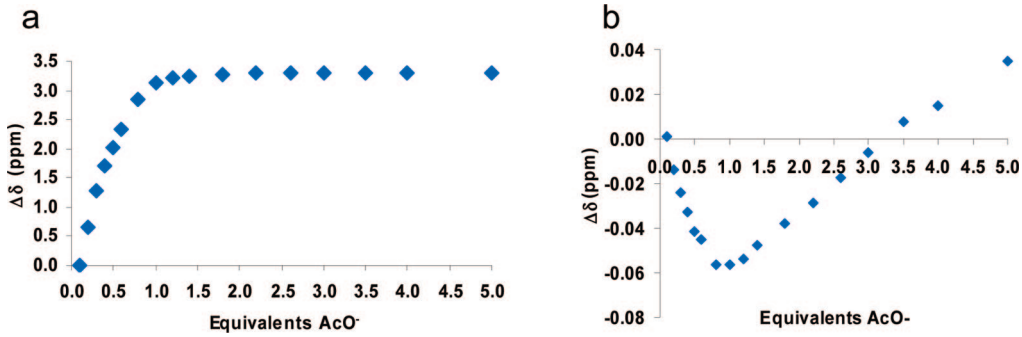

FIGURE 12. (a) Changes in the H1 resonance of **2** (as $\Delta\delta$) upon titration with AcO^-. Similar changes were observed for the H2 proton. (b) Changes seen for the NH3 resonance during the same titration. [Please note change in scale between (a) and (b).]

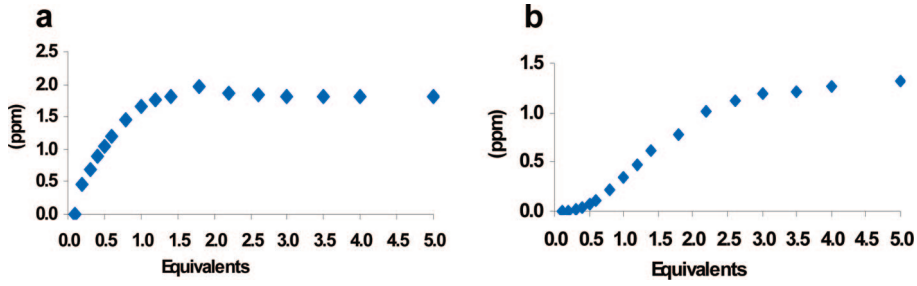

FIGURE 13. (a) Changes in the H1 resonance of **2** (as $\Delta\delta$) upon titration with $H_2PO_4^-$. Similar changes were observed for the H2 proton. (b) The changes seen for the H3 resonance during the same titration.

theory that the first anion recognition activates the amide toward becoming a 'better' hydrogen bonding donor.

Similar results were indeed also seen for **1** (Figure S23, Supporting Information), e.g. the urea protons, being shifted downfield upon anion hydrogen bonding to the anions, while the amide proton was shifted upfield within 0 → 1 equivalents, followed by a subsequent downfield shift after one equivalent of AcO^-. When the same titrations were carried out using $H_2PO_4^-$ (Figure S24 and S25 for **1** and **3**, respectively, Supporting Information), the urea protons of **2** were indeed also shifted downfield, Figure 13a. However, the amide proton was on this occasion, only shifted downfield, and to a much greater extent than previously seen for AcO^-, for example, ~1.2 ppm, Figure 13b. Furthermore, the changes were only minor within the 0 → 1 equivalent range, but significant changes occurred thereafter, up to ca. 3 equivalents. Again, these results confirm the results observed previously from the absorption titrations, and demonstrate that a significant activation occurs for the amide proton after the initial anion binding at the urea moiety.

In contrast to the above results, receptor **3**, gave rise to homogeneous changes for all of the N−H protons upon titration with AcO^-, Figure 14, where all the protons were engaged in the initial binding of the anion, and no significant changes were observed in the ^{1}H NMR for NH1-NH3 after the 1:1 binding stoichiometry (Figure S26, Supporting Information). Again, this is in agreement with that observed for the changes observed in

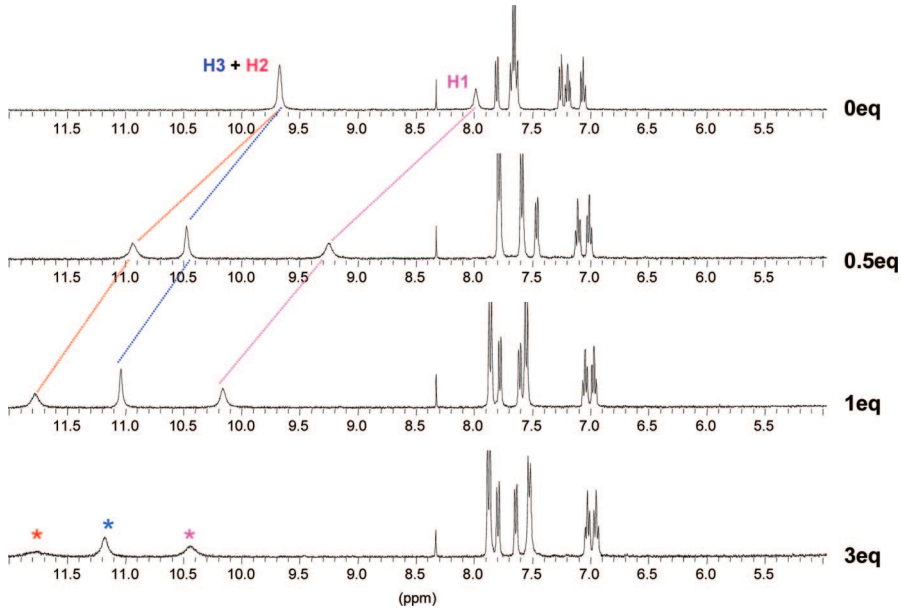

FIGURE 14. Stack plot of the ^{1}H NMR (400 MHz, DMSO-d_6) spectra of **3** upon addition of 0, 0.5 1 and 3 equivalents of $H_2PO_4^-$.

the absorption spectra of **3**, where only the 1:1 binding was observed. As was seen before, the recognition of Cl^- was also clearly observed in the ^{1}H NMR, however, the gradual changes observed, >4 equiv reflected the weaker affinity for this anion (Figure S27 and S28, Supporting Information).

From these ^{1}H NMR titration studies, it can be concluded that: (i) the nature of the changes in the amide N−H proton and the magnitude of the chemical shift is both dependent on the ring substitution pattern, as well as the nature of the anion and that (ii) particularly for both **1** and **2**, the initial anion binding interaction at the urea site enhances the binding ability of the amide proton, which we describe as the consequence of "positive allosteric effect".[25]

Conclusion

Herein we have developed three new anion receptors **1**−**3**, based on the use of combined aryl amide and urea functionalities as hydrogen bonding donors. All three ligands produced crystals that were suitable for X-ray crystal structure analysis. These showed that the location of the amide relative to the urea moiety played a major role in their ability to form large solid state networks through the formation of either intra- or intermolecular hydrogen bonding interactions.

All the receptors were found to interact strongly with anions such as AcO^-, $H_2PO_4^-$, $H_2P_2O_7^{2-}$ and F^- in CH_3CN, as determined by the changes in their respective absorption spectra. While **3** gave rise to 1:1 binding stoichiometries of these anions, occurring through hydrogen bonding of the anions to both the amide and the urea protons, we demonstrated that this 'first' hydrogen bonding interaction in receptors **1** and **2**, leads to activation of the amide moiety, which in turn is able to participate in hydrogen bonding interactions with a second equivalent of these anions. This we describe as being the consequence of positive allosteric effects in these two structures, a phenomenon not much explored to date for supramolecular anion recognition or sensing.

We further demonstrated that this second binding interaction/activation by carrying out ^{1}H NMR titrations in DMSO-d_6, and observing the changes observed in the resonance of the three N−H protons. On all occasions, using AcO^- and $H_2PO_4^-$, the two urea protons were significantly shifted downfield upon binding to the receptor; however, the amide proton was also affected, being most pronounced for the binding of $H_2PO_4^-$. Importantly, the changes in the amide protons were most affected after the addition of one equivalent of these anions, demonstrating that in both **1** and **2**, the amide N−H was directly involved in anion coordination. In contrast, only 1:1 binding was seen for the recognition of these anions by **3**. To the best of our knowledge, we have demonstrated for the first time that simple urea-amido derivatives can participate in anion recognition chemistry, where the recognition of an anion gives rise to stronger affinity for the binding of the second species. We are currently investigating the properties of these, and related compounds in greater detail.

Experimental Section

General Experimental Procedure for Compounds 1−3. The relevant amino acetamide (**10**−**12**) was placed in a 10 mL RBF and dissolved with $CHCl_3$. Trifluoro-*p*-tolyl isocyanate **13** (1.1 equiv) was added, and the solution was then stirred at room temperature overnight under an argon atmosphere. The resulting precipitate was filtered and washed with cold $CHCl_3$. The obtained solid was then dried under vacuum followed by crystallization.

***N*-{4-[3-(4-Trifluoromethyl-phenyl)-ureido]-phenyl}-acetamide (1).** Receptor **1** was synthesized according to above procedure, using *N*-(4-amino-phenyl)-acetamide (see Supporting Information) (0.20 g, 1.33 mmol) and trifluoro-*p*-tolyl isocyanate (0.27 g, 14.6 mmol). The product was isolated and recrystallized from a mixture of $CHCl_3$:CH_3OH to yield the pure compound as an off-white solid (0.405 g, 90% yield). mp decompose above 300 °C; Required for $C_{16}H_{14}F_3N_3O_2$: C, 56.97; H, 4.18; N, 12.46%; Found: C, 56.63; H, 4.12; N, 12.26%; Calculated for $C_{16}H_{14}N_3O_2F_3Na$ m/z = 360.0936 [M + Na]. Found m/z = 360.0939; ^{1}H NMR (400 MHz, d_6-$(CD_3)_2SO$) δ_H: 9.87 (broad s, 1H, NH), 9.05 (broad s, 1H, NH), 8.71 (s, 1H, NH), 7.64 (d, 4H, CH, J = 9.00 Hz), 7.50 (d, 2H, CH, J = 9.04 Hz), 7.38 (d, 2H, CH, = 9.04 Hz), 2.02 (s, 3H, CH_3); ^{13}C NMR (100 MHz, d_6-$(CD_3)_2SO$) δ_C: 167.9, 152.3, 143.5, 134.5, 134.1, 126.1, 125.9, 119.6, 118.9, 117.7, 23.8; ^{19}F NMR (376 MHz, d_6-$(CD_3)_2SO$) δ_F: −60.5 (CF_3); MS (ES^+) m/z: 360.09 [M + Na]; IR υ_{max} (cm^{-1}) 3330, 3275, 3144, 3089, 1693, 1647, 1605, 1546,

1512, 1403, 1318, 1303, 1242, 1214, 1185, 1162, 1102, 1066, 1015, 969, 839, 824, 788, 757, 670.

***N*-{3-[3-(4-Trifluoromethyl-phenyl)-ureido]-phenyl}-acetamide (2).** Receptor **2** was synthesized according to above procedure using *N*-(3-amino-phenyl)-acetamide (see Supporting Information) (0.09 g, 0.57 mmol) and trifluoro-*p*-tolyl isocyanate (0.12 g, 0.62 mmol). The product was isolated and recrystallized from a mixture of CH_3CN:H_2O to yield the pure compound as an off-white solid (0.133 g, 70% yield). mp 202−205 °C; Required for $C_{16}H_{14}F_3N_3O_2.H_2O$: C, 54.09; H, 4.54; N, 11.83%; Found: C, 53.66; H, 4.40; N, 11.76%; Calculated for $C_{16}H_{14}N_3O_2F_3Na$ *m*/*z* = 360.0936 [M + Na]. Found *m*/*z* = 360.0947; ^{1}H NMR (400 MHz, d_6-$(CD_3)_2SO$) δ_H: 9.95 (broad s, 1H, NH), 9.04 (broad s, 1H, NH), 8.87 (broad s, 1H, NH), 7.79 (s, 1H, CH), 7.65 (d, 4H, CH, *J* = 9.00 Hz), 7.20 (m, 3H, CH), 2.04 (s, 3H, CH_3); ^{13}C NMR (100 MHz, d_6-$(CD_3)_2SO$) δ_C: 168.4, 152.2, 143.5, 139.8, 139.57, 129.0, 126.1, 126.1, 125.9, 123.2, 121.9, 121.5, 117.8, 113.0, 112.9, 108.9, 24.0;^{19}F NMR (376 MHz, d_6-$(CD_3)_2SO$) δ_F: −60.5 (CF_3); MS (ES^+) *m*/*z*: 338.13 [M + H], 360.09 [M + Na]; IR υ_{max} (cm^{-1}) 3299, 1640, 1599, 1545, 1441, 1408, 1327, 1292, 1222, 1165, 1128, 1107, 1067, 1016, 964, 880, 841, 779, 750, 690.

***N*-{2-[3-(4-Trifluoromethyl-phenyl)-ureido]-phenyl}-acetamide (3).** Receptor **3** was synthesized according to above procedure using *N*-(2-amino-phenyl)-acetamide (see Supporting Information) (0.08 g, 0.53 mmol), and trifluoro-*p*-tolyl isocyanate (0.10 g, 0.54 mmol). The product was isolated and recrystallized from a mixture of $CHCl_3$:CH_3OH to yield the pure compound as a white solid (0.159 g, 88% yield). mp 204−206 °C; Required for $C_{16}H_{14}F_3N_3O_2$.1/4 CHCl3: C, 53.16; H, 3.91; N, 11.44%; Found: C, 53.50; H, 3.88; N, 11.54%; Calculated for $C_{16}H_{14}N_3O_2F_3Na$ *m*/*z* = 360.0936 [M + Na]. Found *m*/*z* = 360.0940; ^{1}H NMR (400 MHz, d_6-$(CD_3)_2SO$) δ_H: 9.68 (s, 1H, NH), 9.66 (s, 1H, NH), 7.99 (s, 1H, NH), 7.81 (d, 1H, CH, *J* = 8.52 Hz), 7.66 (d, 4H, CH, *J* = 8.52 Hz), 7.26 (d, 1H, CH, *J* = 8.04 Hz), 7.19 (t, 1H, CH, *J* = 7.52 Hz, 8.00 Hz), 7.06 (t, 1H, CH, *J* = 8.04 Hz, 7.52 Hz), 2.11 (s, 3H, CH_3); ^{13}C NMR (100 MHz, d_6-$(CD_3)_2SO$) δ_C: 169.3, 152.4, 143.6, 133.2, 128.7, 121.8, 121.5, 126.1, 125.9, 125.8, 123.2, 122.9, 117.7, 23.3; ^{19}F NMR (376 MHz, d_6-$(CD_3)_2SO$) δ_F: −60.54 (CF_3); MS (ES^+) *m*/*z*: 360.09 [M + Na]; IR υ_{max} (cm^{-1}) 3253, 3188, 3123, 3053, 1678, 1649, 1605, 1542, 1503, 1475, 1440, 1408, 1316, 1248, 1165, 1108, 1067, 1042, 1015, 969, 951, 849, 821, 746, 673.

X-Ray Crystallography. The data for crystal **1** was collected on a Bruker Smart Apex Diffractometer.[23] A suitable crystal was selected and mounted using inert oil on a 0.30 mm quartz fiber tip and immediately placed on the goniometer head in a 123 K N2 gas stream. The data was collected using Bruker Smart Version 5.625 software run in multirun mode and 2400 image frames, of 0.3° per frame, were recorded. Data integration and reduction were carried out using Bruker Saint+ Version 6.45 software and corrected for absorption and polarization effects using Sadabs Version 2.10 software.

The data for crystals **2** and **3** were collected on a Rigaku Saturn 724 CCD Diffractometer. Suitable crystals from each compound were selected and mounted using an inert oil on a 0.30 mm quartz fiber tip and immediately placed on the goniometer head in a 103K N2 gas stream. The data sets were collected using Crystalclear-SM 1.4.0 software and 1680 diffraction images, of 0.5° per image, were recorded. Data integrations, reductions and corrections for absorption and polarization effects were all performed using Crystalclear-SM 1.4.0 software. Space group determinations, structure solutions and refinements were obtained using Crystalstructure ver. 3.8 and Bruker Shelxtl Ver. 6.14 software. Thse structures are also shwon in Figures S29−S31 (Supporting Information), drawn with ellipsoids drawn at the 50% probability level.

Crystal Data 1. $C_{16}H_{14}F_3N_3O_2$, M = 337.3, Monoclinic, a = 11.9903(12), b = 7.6035(8), c = 17.4995(18) Å, β = 105.585(2)°, U = 1536.7(3)Å^3, T = 123 K, space group P2(1)/c, Z = 4, μ (Mo Kα) = 0.123 mm^{-1}, 11791 reflections collected, 2701 unique, (R_{int} = 0.0560), R = 0.0477, $wR2$ [$I > 2\sigma(I)$] = 0.1048, CCDC deposition number 692270.

Crystal Data 2. $C_{17}H_{17}F_3N_3O_3$, M = 369.34, Triclinic, a = 4.649(3), b = 6.738(5), c = 13.324(10) Å, α = 87.993(13)°, β = 89.247(17)°, γ = 88.20(2)°, U = 416.9(5)Å^3, T = 103 K, space group P1, Z = 1, μ (Mo Kα) = 0.124 mm^{-1}, 8994 reflections collected, 4404 unique, (R_{int} = 0.0316), R = 0.0520, $wR2$ [$I > 2\sigma(I)$] = 0.1331, CCDC deposition number 692269.

Crystal Data 3. $C_{64}H_{56}F_{12}N_{12}O_8$, M = 1349.21, Monoclinic, a = 11.322(17), b = 15.80(2), c = 8.821(12)Å, β = 96.43(3)°, U = 1568(4)Å^3, T = 103 K, space group P2(1)/c, Z = 1, μ (Mo Kα) = 0.120 mm^{-1}, 7829 reflections collected, 2765 unique, (R_{int} = 0.102), R = 0.0843, $wR2$ [$I > 2\sigma(I)$] = 0.2287, CCDC deposition number 651190.

NMR Titrations. The experiments were carried out by using a known amount of the host dissolved in 0.8 mL of solvent ([host] ≈ 7.4 × 10^{-3} M). The anion guest solutions were prepared such that 5 μL of the solution would give 0.1 equivalents of anion ([anion] ≈ 1.2 × 10^{-1} M). After each addition of the anion guest to the NMR tubes, the ^{1}H NMR spectra was recorded (400 MHz) after 5 min equilibration.

Acknowledgment. We thank IRCSET (Basic Research Grant) and TCD (Postgraduate Award to C.M.G.d.S.) for financial support. We thank Dr. John E. O'Brien for assisting with recording NMR and Dr. Emma B. Veale for her suggestions and valuable comments during the writing of this manuscript.

Supporting Information Available: General experimental description, synthesis and characterization of all intermediates, ^{1}H, ^{13}C and ^{19}F NMRs spectra of all intermediates and final products. This material is available free of charge via the Internet at http://pubs.acs.org.

JO8014424